Journal of Inorganic Biochemistry 108 (2012) 15–21

Contents lists available at SciVerse ScienceDirect

Journal of Inorganic Biochemistry

journal homepage: www.elsevier.com/locate/jinorgbio

Bio-inspired flavonol and quinolone dioxygenation by a non-heme iron catalyst modeling the action of flavonol and 3-hydroxy-4(1*H*)-quinolone 2,4-dioxygenases

József S. Pap [a], Andrea Matuz [a], Gábor Baráth [a], Balázs Kripli [a], Michel Giorgi [b], Gábor Speier [a], József Kaizer [a,*]

[a] Department of Chemistry, University of Pannonia, 8201 Veszprém, Hungary
[b] Aix-Marseille Université, FR1739, Spectropole, Campus St. Jérôme, Avenue Escadrille Normandie-Niemen, 13397 Marseille cedex 20, France

ARTICLE INFO

Article history:
Received 30 August 2011
Received in revised form 27 October 2011
Accepted 15 November 2011
Available online 29 November 2011

Keywords:
Iron complexes
Flavonols
Quinolones
Dioxygenation
Kinetics and mechanism

ABSTRACT

The mononuclear complex, Fe^{III}(*O*-bs)(salen) (salenH_2 = 1,6-bis(2-hydroxyphenyl)-2,5-diaza-hexa-1,5-diene; *O*-bsH = *O*-benzoylsalicylic acid) was synthesized as synthetic enzyme-depside complex, and characterized by spectroscopic methods and X-ray crystal analysis. The dioxygenation of flavonol (flaH) and 3-hydroxy-4-quinolone (quinH_2) derivatives in the presence of catalytic amounts of Fe^{III}(*O*-bs)(salen) results in the oxidative cleavage of the heterocyclic ring to give the corresponding *O*-benzoylsalicylic and anthranilic acid derivatives with concomitant release of carbon monoxide. These reactions can be regarded as biomimetic functional models with relevance to the iron-containing flavonol and the cofactor-independent 3-hydroxy-4(1*H*)-quinolone 2,4-dioxygenases.

1. Introduction

Ring cleavage is the crucial step in the microbial degradation of aromatic and heterocyclic compounds. Flavonoids (flaH, **1**,**2**) are polyphenolic pigments found in higher plants and some fungi (Scheme 1) [1,2]. Current interest in the compounds of flavonoid group is explained by their varied biological activity, with antioxidant, antiradical, antimicrobial, hepatoprotective, anti-inflammatory and other interesting properties [3–7]. In a clinical study, the risk of coronary heart disease was shown to correlate inversely with the extent of flavonoid intake [8]. 2-Methylquinoline utilization by the soil bacterium *Arthrobacter nitroguajacolicus* Rü61a involves two initial hydroxylation steps to form 2-methyl-3-hydroxy-4(1*H*)-quinolone (2Me-quinH_2, **3**) [9]. *Pseudomonas putida* 33/1 utilizes 3-hydroxy-4(1*H*)-quinolone (quinH_2, **4**) as sole source of carbon, nitrogen, and energy [10]. These substrates with the 2-phenyl derivatives (PhquinH_2, **5** and 1Me-PhquinH_2, **6**) structurally are isoelectronic with flavonols. 2-Alkyl-4(1*H*)-quinolones are known as secondary metabolites of fluorescent pseudomonads, exhibiting antimicrobial activity primarily towards Gram-positive bacteria [11]. 2-Heptyl-3-hydroxy-4(1*H*)-quinolone was later found to act as one of the signaling molecules in the quorum sensing sytem of the opportunistic pathogen *Pseudomonas aeruginosa*, and therefore was named *Pseudomonas* quinolone signal (PQS) [12]. PQS is involved in the regulation of the biosynthesis of many virulence factors, and it affects biofilm development and cellular fitness. It also acts as an iron trap, sequestering iron from the environment [13,14].

Flavonols are readily degraded by microorganisms. The copper- and iron-containing flavonol 2,4-dioxygenases (quercetinases) catalyze the oxidative degradation of flavonol(s) to depside(s) (phenolic carboxylic acid ester(s)) and carbon monoxide by fungi like *Aspergillus flavus* [15], *Aspergillus niger* [16], *Aspergillus japonicus* [17] and the protein YxaG from *Bacillus subtilis* [18–20] (Eq. (1)).

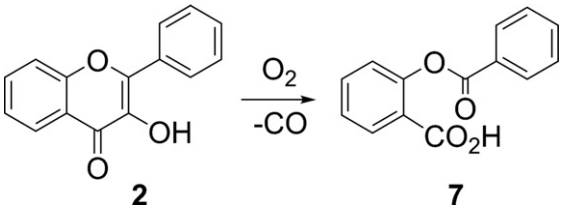

2 **7** (1)

Ring opening reaction of 2-methyl-3-hydroxy-4(1*H*)-quinolone (**3**) and 3-hydroxy-4(1*H*)-quinolone (**4**) to *N*-acetylanthranilic (**8**) and *N*-formylanthranilic acid (**9**), including CO release, is catalyzed by 1*H*-3-

* Corresponding author. Fax: +36 88624469.
E-mail address: kaizer@almos.vein.hu (J. Kaizer).

0162-0134/$ – see front matter © 2011 Elsevier Inc. All rights reserved.
doi:10.1016/j.jinorgbio.2011.11.013

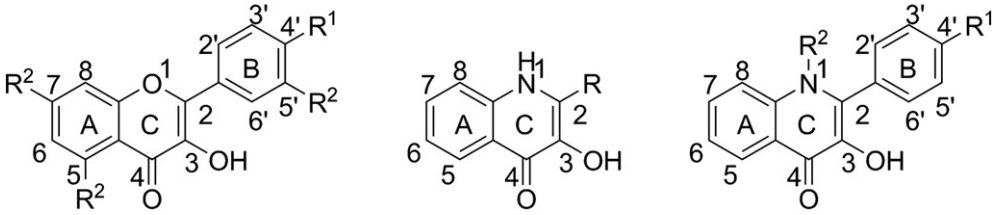

1; $R^1 = R^2 = OH$
2a; $R^1 = R^2 = H$
2b; $R^1 = NMe_2$, $R^2 = H$
2c; $R^1 = OMe$, $R^2 = H$
2d; $R^1 = Me$, $R^2 = H$
2e; $R^1 = Cl$, $R^2 = H$
2f; $R^1 = CN$, $R^2 = H$

3; R = Me
4; R = H

5a; $R^1 = R^2 = H$
5b; $R^1 = OMe$, $R^2 = H$
5c; $R^1 = Br$, $R^2 = H$
5d; $R^1 = NO_2$, $R^2 = H$
6; $R^1 = H$, $R^2 = Me$

Scheme 1. Structure and substitution pattern of the applied model substrates.

hydroxy-4-oxoquinoline 2,4-dioxygenase (QDO) and 1*H*-3-hydroxy-4-oxoquinaldine 2,4-dioxygenase (HDO) (Eq. (2)) [11,21–25].

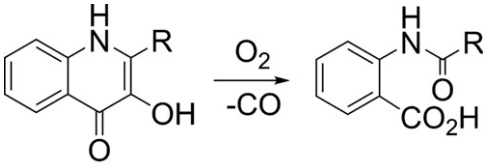

3; R = Me
4; R = H

8; R = Me
9; R = H

(2)

Model studies of FDOs have demonstrated that autoxidations of potassium, zinc, iron, manganese, and copper flavonolates, mainly at elevated temperatures, have resulted in enzyme-like products [26–31]. Mononuclear iron(III) flavonolate complex Fe^{III}(fla)(salen) was synthesized as synthetic enzyme-substrate complex, and its direct and carboxylate-enhanced dioxygenation was investigated in detail. It was shown that bulky carboxylates as coligands dramatically enhance the reaction rate, which can be explained by two different mechanisms, caused by the formation of more reactive monodentate iron(III) flavonolate complexes [32]. Evidence for direct electron transfer from the flavonolate ligand to dioxygen to form superoxide radical anion was proved by the superoxide scavenger nitroblue tetrazolium (NBT) [32].

The base-catalyzed dioxygenation of 1*H*-3-hydroxy-4-quinolone derivatives leads to the corresponding cleavage products derived from either an endoperoxide or a 1,2-dioxetane intermediate. A persistent 1*H*-2-phenyl-3-oxy-4-quinolone radical could also be detected by EPR [33].

In this study we present the synthesis and structural characterization of the first iron-containing synthetic enzyme-depside complex, Fe^{III}(*O*-bs)(salen) (**10**), that highly selectively catalyzes the dioxygenation of flavonol and quinolone derivatives, mimicking the action of 2,4-dioxygenases.

Table 1
Summary of the crystallographic data and structure parameters for Fe^{III}(*O*-bs)(salen).

Formula weight	1198.85
Crystal system	Monoclinic
Crystal description	Prism
Space group	P2/n
Unit cell dimensions	
a (Å)	22.5007(3)
b (Å)	10.1645(1)
c (Å)	25.5072(4)
α (°)	90.00
β (°)	107.537(1)
γ (°)	90.00
Volume (Å^3)	5562.57(13)
Z	4
Calculated density (g cm^{-1})	1.432
Crystal size (mm^3)	0.4 × 0.25 × 0.25
Index ranges	$0 \le h \le 30$
	$0 \le k \le 13$
	$-34 \le l \le 32$
Temperature (K)	203(2)
Radiation	MoK_α(λ = 0.71073)
Absorption coefficient (mm^{-1})	0.592
F (0 0 0)	2496
Reflections collected	13979
Observed reflections	8858
[$I > 2\sigma(I)$]	
Goodness-of-fit	1.028
Final *R* indices	$R_1 = 0.0711$[a], w$R_2 = 0.1463$[b]
R indices (all data)	$R_1 = 0.1258$, w$R_2 = 0.1766$

[a] $R_1 = \Sigma||F_o| - |F_c||/\Sigma|F_o|$. [b] $wR_2 = [\Sigma w(F_o^2 - F_c^2)^2/\Sigma w(F_o^2)^2]^{1/2}$.

2. Experimental

2.1. Materials

All manipulations were performed under a pure argon atmosphere using standard Schlenk-type inert-gas techniques unless otherwise stated. Solvents used for the reactions were purified by literature methods and stored under argon. Flavonol [34], 4′-methyl- [35], 4′-methoxy- [34], 4′-chloro- [35], 4′-cianoflavonol [35], 1-methyl-2-phenyl-3-hydroxy-4-quinolone (**6**) [36], 2-phenyl-3-hydroxy-4(1*H*)- quinolone [36], 4′-bromo-, 4′-methoxy-, 4′-nitro-2-phenyl-3-hydroxy-4(1*H*)- quinolone [36], 2-methyl-3-hydroxy-4(1*H*)-quinolone [36], and *O*-benzoylsalicylic acid were prepared according to published procedures [37]. Diazomethane was freshly prepared according to the literature in ether and immediately used for the methylation reactions [38]. The complex Fe^{III}(salen)Cl was synthesized as it was published earlier [39]. All other

Table 2
Selected bond lengths (Å) and bond angles (deg) for Fe^{III}(*O*-bs)(salen).

N(1)–Fe(1)	2.131(3)	N(2)–Fe(1)	2.086(3)
O(1)–Fe(1)	1.897(2)	O(2)–Fe(1)	1.912(2)
O(3)–Fe(1)	2.156(2)	O(4)–Fe(1)	2.106(2)
O(4)–C(17)	1.266(4)	O(3)–C(17)	1.256(4)
O(2)–C(16)	1.317(4)	O(1)–C(1)	1.324(4)
C(23)–O(5)	1.401(4)	O(5)–C(24)	1.363(4)
C(24)–O(6)	1.203(4)	C(24)–C(25)	1.481(6)
O(1)–Fe(1)–N(2)	161.33(12)	O(4)–Fe(1)–N(1)	142.59(10)
O(4)–Fe(1)–O(3)	61.06(9)	O(2)–Fe(1)–O(3)	152.81(10)
Fe(1)–O(4)–C(17)	91.29(19)	Fe(1)–N(2)–C(9)	113.1(2)

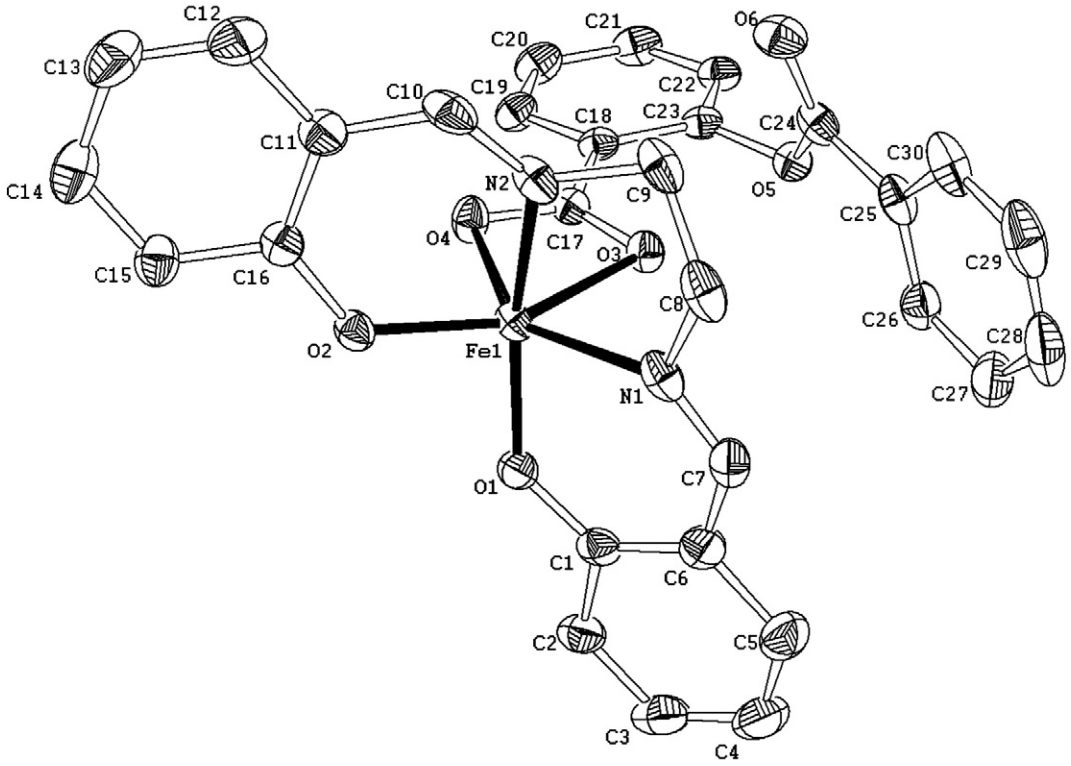

Fig. 1. Molecular structure of **10**. Ellipsoids are plotted at the 50% probability level.

chemicals were commercial products and were used without further purification.

2.2. Analytical and physical measurements

Infrared spectra were recorded on an Avatar 330 FT-IR Thermo Nicolet instrument using samples in KBr pellets. UV–vis spectra were recorded on an Agilent 8453 diode–array spectrophotometer using quartz cells (data are summarized in chapter 2.3). GC analyses were performed on a Hewlett Packard 5830A gas chromatograph equipped with a flame ionization detector and a CP SIL 8CB column. Microanalyses were done by the Microanalytical Service of the University of Pannonia. Cyclic voltammograms (CV) were taken on a VoltaLab 10 potentiostat with VoltaMaster 4 software for data process. The electrodes were as follows: glassy carbon (working), Pt wire (auxiliary), and Ag/AgCl with 3 M KCl (reference). The potentials were referenced *vs.* the ferrocene/ferrocenium (Fc/Fc^+) redox couple. CVs were measured in argon saturated DMF using 0.1 M tetrabuthylammonium perchlorate (TBAP) salt as electrolyte. The crystal evaluations and intensity data collections for Fe^{III}(*O*-bs)(salen) (**10**), were performed on a Bruker–Nonius Kappa CCD single-crystal diffractometer using Mo Kα radiation (λ = 0.71073 Å) at 203(2) K. Crystallographic data and details of the structure determination are given in Table 1, whereas elected bond lengths and angles are listed in Table 2. SHELX-97 [40] was used for structure solution and full matrix least squares refinement on F^2. CIF files are available in the CCDC database (CCDC 824209).

2.3. Synthesis of Fe^{III}(*O*-bs)(salen) (**10**)

A solution of 0.57 g (1.6 mmol) of Fe^{III}(salen)Cl and 0.38 g (1.6 mmol) of *O*-bsH in 10 mL MeOH was stirred at room temperature

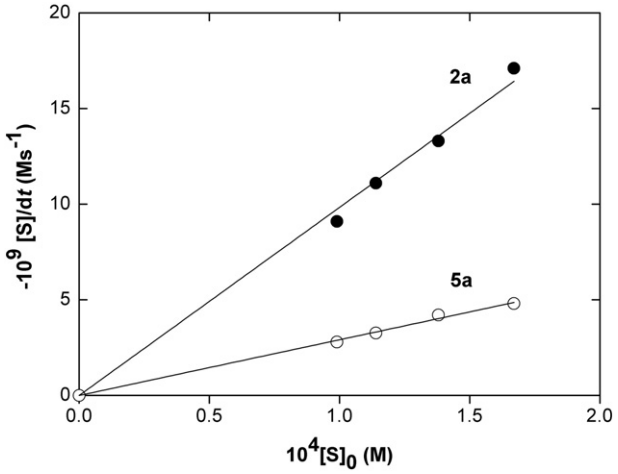

Fig. 2. Dependence of the initial rates on the initial concentration of **2a** (Table S1, exp. 4–7) and **5a** (Table S2, exp. 4–7).

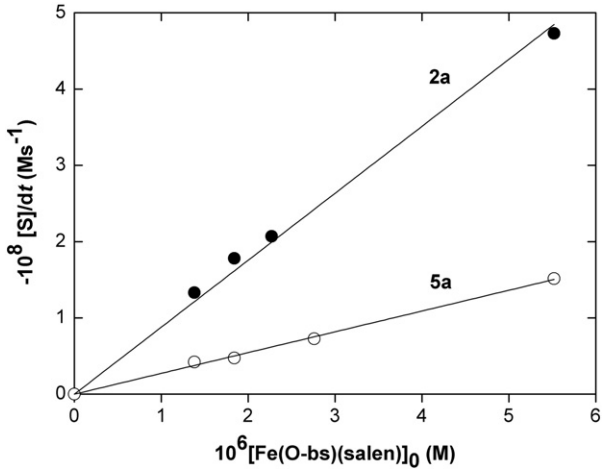

Fig. 3. Dependence of the initial rates on the concentration of Fe^{III}(*O*-bs)(salen) for **2a** (Table S1, exp. 4, 8–10) and **5a** (Table S2, exp. 4, 8–10).

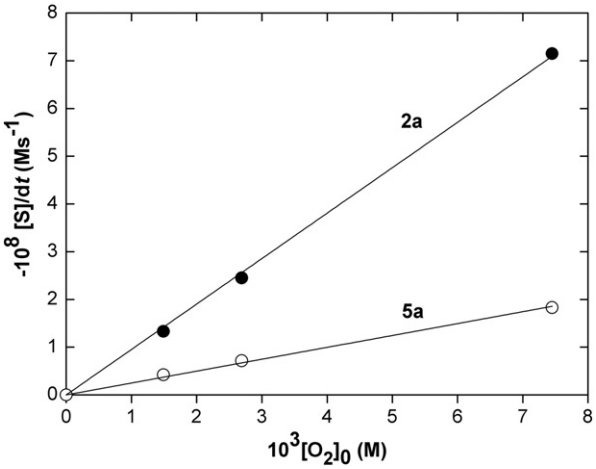

Fig. 4. Dependence of the initial rates on the dioxygen concentration for **2a** (Table S1, exp. 4, 11–12) and **5a** (Table S2, exp. 4, 11–12).

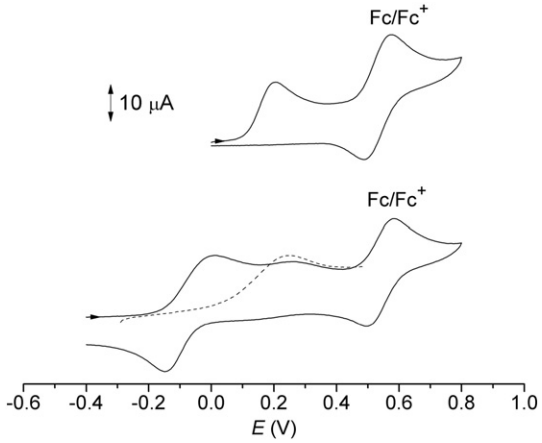

Fig. 5. CVs of anions from **2a** (top), **5a** (bottom) and 4′H-Phquin$_{ox}$ (dashed line), 1 mM in DMF containing ~1 mM ferrocene as internal standard, at 100 mV/s scan rate. Voltammograms are plotted against the Ag/AgCl reference electrode.

under argon. After 30 min 220 μL (1.6 mmol) of triethylamine was added drop-wise. The mixture was stirred for 1 h, the solvent was evaporated in a vacuum, and the residue was washed with cold methanol and diethylether and vacuum-dried. Yield: 0.39 g (69%). Anal. Calcd for $C_{30}H_{23}N_2O_6Fe$: C, 63.96; H, 4.12; N, 4.97. Found: C, 63.78; H, 4.17; N, 4.85. FT-IR bands (KBr pellet, cm^{-1}): 3188 m, 3010 m, 2925 m, 1731 s, 1629 s, 1597 s, 1512 s, 1445 m, 1385 m, 1327 w, 1294 m, 1200 m, 1034 s, 905 m, 923 759 s, 618 m, 425 w. Crystals suitable for X-ray structural determination were obtained from dichloromethane.

2.4. Catalytic oxygenation of flavonol, or 2-phenyl-3-hydroxy-4(1H)-quinolone catalyzed by Fe^{III}(O-bs)(salen)

100 mg (0.42 mmol) of flavonol (2-phenyl-3-hydroxy-4(1*H*)-quinolone) and 9 mg (0.017 mmol) of Fe^{III}(*O*-bs)(salen) were dissolved and stirred at 100 °C in 5 mL DMF for 15 h under dioxygen atmosphere. Diazomethane solution (2 mL) was added to 0.2 mL of the reaction mixture at r.t. and the conversion of flavonol into *O*-benzoylsalicylic acid (75%), or 2-phenyl-3-hydroxy-4(1*H*)-quinolone into *N*-benzoylanthranilic acid (64%) was determined by GC as methylated derivatives in the presence of benzoin as internal standard. The formation of CO was proved by GC analysis of the gas phase (~70 and ~60%, respectively).

2.5. Kinetic measurements

The Fe^{III}(*O*-bs)(salen)-catalyzed oxygenation of flavonol or 2-phenyl-3-hydroxy-4(1*H*)-quinolone was followed by UV–vis spectroscopy. In a typical experiment flavonol or 2-phenyl-3-hydroxy-4(1*H*)-quinolone and Fe^{III}(*O*-bs)(salen) was dissolved under argon atmosphere in a thermostated reaction vessel with an inlet for taking samples with a syringe, and connected to mercury manometer to regulate constant dioxygen pressure. The solution was then heated to appropriate temperature and the argon was replaced with dioxygen. The concentration of flavonol or 2-phenyl-3-hydroxy-4(1*H*)-quinolone was determined by measuring the absorbance of the reaction mixture at 343 or 372 nm [log ε 4.24 or log ε 3.96]. Experimental conditions are summarized in Tables S1 and S2. The dioxygen concentration in DMF was calculated from literature data taking into account the partial pressure of DMF [41] and assuming the validity of Dalton's law [42].

Table 3
Kinetic data for the Fe^{III}(*O*-bs)(salen)-catalyzed dioxygenation of flavonol and 3-hidroxy-quinolone derivatives in DMF.

	10^4k[a] M^{-2} s^{-1}	$E_A^{\neq}$ kJ mol^{-1}	$\Delta H^{\neq}$ kJ mol^{-1}	$\Delta S^{\neq}$ J mol^{-1} K^{-1}	σ
2a	4.82 ± 0.15	53 ± 2	50 ± 2	−27 ± 1	0.37
3	2.65 ± 0.09	–	–	–	–
5a	1.36 ± 0.04	60 ± 4	57 ± 4	−20 ± 2	0.75
6	1.63 ± 0.06	58 ± 4	55 ± 4	−20 ± 1	–

[a] In DMF at 110 °C.

3. Results and discussion

*3.1. Synthesis and characterization of the Fe^{III}(O-bs)(salen) (**10**)*

As a synthetic enzyme-depside model (*O*-benzoylsalicylato)iron(III) complex was prepared by the reaction of equimolar amounts of Fe^{III}(salen)Cl and *O*-benzoylic acid in the presence of triethylamine in methanol. Complex **10** isolated as a brown solid is stable in air and analyzed satisfactorily for C, H, N. The infrared (IR) spectrum of the complex shows ν(CO) and $\nu(CO_2)$ bands corresponding to the coordinated *O*-benzoylsalicylate at 1731, and 1544, 1385 cm^{-1}, respectively. The difference between the asymmetric and symmetric stretching frequencies of this carboxylato group [$\Delta\nu = \nu_{as}(CO_2) - \nu_s(CO_2)$] is 159 cm^{-1}, rendering these to a bidentate bonding mode [43,44]. Crystals of complex **10** of X-ray quality were obtained from dichloromethane. Crystallographic characterization has shown that the geometry around the six-coordinated iron(III) center is distorted octahedral, and that the *O*-benzoylsalicylate anion is coordinated as a bidentate ligand with a strongly twisted conformation of the salen ligand. A view of the coordination geometry is given in Fig. 1. The Fe(1) – O(3) bond is only 0.040 Å longer than the Fe(1) – O(4) bond.

*3.2. Catalytic dioxygenation of flavonol and 3-hydroxy-quinolone derivatives catalyzed by Fe^{III}(O-bs)(salen) (**10**)*

The dioxygenation reaction of flaH and PhquinH_2 with dioxygen in the presence of a catalytic amount of Fe^{III}(*O*-bs)(salen) was performed in DMF solution and examined at 100 °C with a ratio of 1:25 between initial concentration of the iron complex and the corresponding substrate (**2a** or **5a**). We have found that the dioxygenation of **2a** and **5a** results in oxidative cleavage of the heterocyclic ring to give *O*-benzoylsalicylic acid (75%) and *N*-benzoylanthranilic acid (64%) with concomitant release of carbon monoxide. The dioxygenation reaction in both cases was selective, no other products were obtained.

Detailed kinetic measurements were carried out for the **2a** and **5a** dioxygenation in DMF solution and examined in the temperature range from 353 to 383 K with a ratio between initial concentrations of Fe^{III}(*O*-bs)(salen) and the substrate in the range 1:20–40. Experiments were

Table 4
Electrochemical data for 4′R-flaH and 4′R-PhquinH$_2$ derivatives and 4′H-Phquin$_{ox}$ in DMF *vs.* the ferrocene internal standard ([*E*] = mV).

4′R-flaH	**2a**	**2a**	**2f**	**2b**	**2e**	**2d**	**2c**		
$E^{\circ\prime}_{pa1}$[a]	−326		−225	−593	−300	−378	−446		
$E^{\circ\prime}_{pc1}$[a]	–		–	–	–	–	–		
4′R-PhquinH$_2$	**5a**						**5b**	**5c**	**5d**
$E^{\circ\prime}_{pa1}$[a]	−527	–					−559	−510	−449
$E^{\circ\prime}_{pc1}$[a]	−693	–					−716	−648	−605
$E^{\circ\prime}_{pa2}$[a]	−292	−291[b]					−321	–	–

[a] ±5 mV.
[b] 4′H-Phquin$_{ox}$.

also carried out at different dioxygen concentrations. Experimental conditions are summarized in Tables S1 and S2. Catalytic reactions were followed by UV–vis spectroscopy by determining the substrate concentration as a function of time under constant dioxygen pressure. The variation of the absorbance was determined for **2a** and **5a** at 343 and 372 nm, respectively. The measured absorption spectra for the catalytic dioxygenation of flavonol at 333 K are shown in Fig. S1, with time range being 2.5 h. Direct electron transfer from the flavonolate ligand to dioxygen to form superoxide radical anion was proved by the reduction of nitroblue tetrazolium (NBT) as superoxide scavenger to blue formazan. By the addition of NBT to the reaction mixture, the yellow color turns to intense green and new intense band at 520 nm arises. This absorption has been assigned to formazan signaling the presence of superoxide anion [45].

The observed initial rates for **2a** and **5a** are compiled in Tables S1 and S2. When dioxygenase activity was studied, flavonol was the more reactive substrate. The estimated initial rates (under the same conditions) were $V_0 = 1.33\times10^{-8}$ Ms^{-1}, and $V_0 = 0.39\times10^{-8}$ Ms^{-1}, respectively, for **2a** and **5a**. Therefore, the flavonol is three-times more reactive than the 2-phenyl-3-hydroxy-4(1*H*)-quinolone, toward dioxygen. In order to determine the rate-dependence on the various reactants catalytic reactions were performed at different substrate, catalyst and dioxygen concentrations (Tables S1 and S2). Initial reaction rates plotted *versus* the initial concentration of substrate (Fig. 2), catalyst (Fig. 3) and dioxygen (Fig. 4) could be fitted with straight lines for both cases establishing a rate law of $-d[\mathbf{2a}\text{ or }\mathbf{5a}]/dt = k_{obs}[\mathbf{2a}\text{ or }\mathbf{5a}][Fe^{III}(O\text{-bs})(salen)][O_2]$, from which a mean value of the kinetic constants of $(4.82\pm0.15)\times10^4$ M^{-2} s^{-1} (**2a**), and $(1.36\pm0.04)\times10^4$ M^{-2} s^{-1} (**5a**), at 333 K were obtained, respectively.

Reaction rate on the catalytic dioxygenation of the 1- and 2-substituted 3-hydroxy-4-quinolone derivatives (1Me-PhquinH (**6**); 2Me-quinH$_2$ (**3**)) under identical conditions were also determined in order to elucidate the role of electronic effects in the reaction rates (Table 3). On the basis of comparison of rate constants at 333 K, these substrates are more reactive than **5a**, suggesting a substrate dependent reactivity order of **2a** > **6** > **3** > **5a**.

Activation parameters calculated for **2a**, **5a** and **6** from temperature-dependence of the reaction rates are $E_A^{\neq} = 53\pm2$ kJ mol^{-1}, $\Delta H^{\neq} = 50\pm2$ kJ mol^{-1}, $\Delta S^{\neq} = -27\pm1$ J mol^{-1} K^{-1}; $E_A^{\neq} = 60\pm4$ kJ mol^{-1}, $\Delta H^{\neq} = 57\pm4$ kJ mol^{-1}, $\Delta S^{\neq} = -20\pm2$ J mol^{-1} K^{-1}; and $E_A^{\neq} = 58\pm4$ kJ mol^{-1}, $\Delta H^{\neq} = 55\pm4$ kJ mol^{-1}, $\Delta S^{\neq} = -20\pm1$ J mol^{-1} K^{-1}, respectively (Table 3). These values are very similar to each other supporting similar, associative-type mechanism (Fig. S2) for the investigated substrates.

3.3. Electrochemical properties of flavonol and 2-phenyl-3-hydroxy-4(1H)-quinolone derivatives

Cyclic voltammetric measurements on the flavonol derivatives in the presence of base have been performed earlier and the irreversible oxidations were associated with the low stability of the generated flavonoxyl radical (4′R-fla$^{\bullet}$) [31]. A correlation between the rate of oxygenation for the potassium flavonolates and their measured E_{pa} values was also established. However, no further details were given on the possible chemical changes accompanying this irreversible electrochemical transition. Now, we have measured the CVs of the various derivatives shown Scheme 1 in DMF under argon, in the presence of an equivalent amount of potassium *tert*-butoxide. In the voltammogram of 4′H-fla$^-$ (Fig. 5, top) an irreversible, one electron oxidation is present at −326 mV *vs.* ferrocene. This transition has been assigned as the one electron oxidation of 4′H-fla$^-$ to 4′H-fla$^{\bullet}$ in the previous study. Very similar CVs were taken with each derivative (potential values are listed in Table 4). The flavonoxyl radical once generated, readily undergoes chemical transformation. We presume that the electrochemical generation of the radical leads to the rapid formation of a dimeric product (Scheme 2) that has been described earlier [46]. This can be accounted for the irreversibility of the electrochemical transition, *e.g.* the absence of $E^{\circ\prime}_{pc1}$.

In contrast with those of the 4′R-fla$^-$ compounds, the CV of 4′H-PhquinH$^-$ (Fig. 5, bottom) exhibits one reversible transition followed by an irreversible oxidation. This behavior is observed for each derivative, although the second oxidation peak is present only as a shoulder

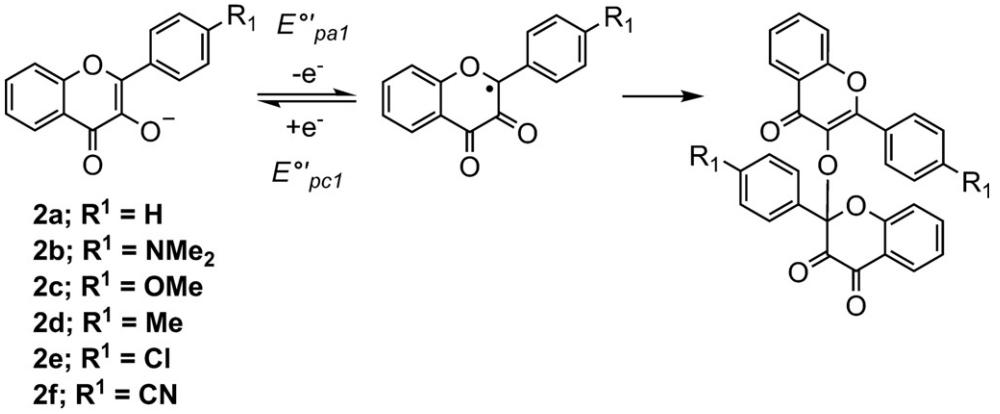

Scheme 2. Formation of the dimeric product upon one-electron oxidation of 4'R-flaH derivatives.

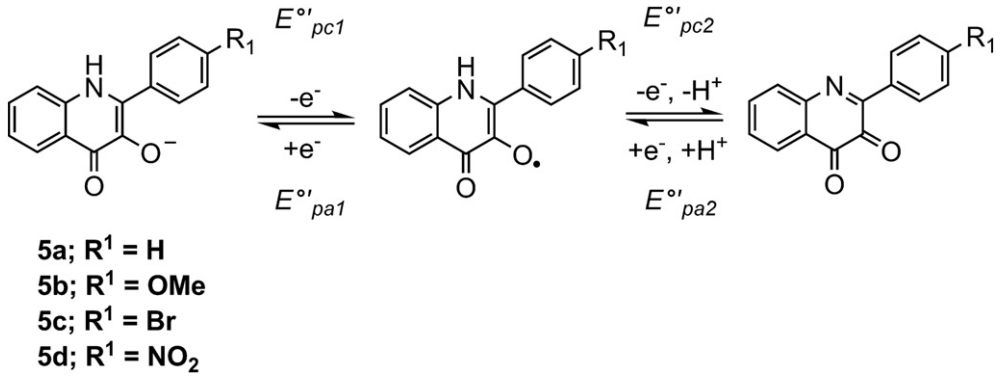

Scheme 3. Proposed products in the one-electron oxidation steps of 4′R-PhquinH derivatives.

of $E^{\circ\prime}_{pa1}$ when R═Br, or NO_2 thus the potential was not determined in these two cases. The potential data and assignments are listed in Table 4. The observed current peaks are associated with the $E^{\circ\prime}_{pa1}$ and $E^{\circ\prime}_{pa2}$ transitions (Scheme 3). The presence of a reverse reduction peak ($E^{\circ\prime}_{pc1}$) is associated with the higher stability of 4′R-PhquinH$^{\bullet}$ radicals that do not undergo chemical changes in the time-scale of the CV experiment. This can be supported by the comparison of $E^{\circ\prime}_{pa1}$ values of the corresponding 4′R-fla^{-} and 4′R-PhquinH^{-} (R═H, or OCH_3) derivatives: the lower potential indicates higher stability for the electrochemically generated radical species in the latter case. The origin of the irreversible $E^{\circ\prime}_{pa2}$ transition was probed by taking the voltammogram of 4′R-Phquin$_{ox}$ (Fig. 5. dashed line) [47] in the oxidation direction from −300 to 500 mV *vs.* the Ag/AgCl electrode. The sole peak that is present coincides with $E^{\circ\prime}_{pa2}$ therefore we tentatively assign this peak as the one-electron process shown in Scheme 3.

The substitution at the 4′R position had a systematic effect on the $E^{\circ\prime}_{pa1}$ potentials that show correlation with Hammett's σ (Fig. 6). This effect can be expected to influence the reaction rates for the oxygenation of these compounds in the presence of the iron complex (Fig. 7). The influence of the 4′R groups on the reaction rate of the catalytic dioxygenation of 4′R-flaH (**2**) and 4′R-PhquinH$_2$ (**5**) showed a linear Hammett plot with a reaction constant of $\rho = -0.37$ and -0.75, respectively, indicating that the electron-releasing groups result in remarkable increase in the reaction rates (Fig. S3). These results suggest that the dioxygen species at the transition state should be electrophilic.

4. Conclusions

In this study we have demonstrated that the complex Fe^{III}(*O*-bs)(salen), which is the first synthetic iron-containing 2,4-FDO enzyme-depside model, highly selectively and efficiently catalyzes the dioxygenolytic cleavage of the heterocycle ring of flavonols and 3-hydroxy-4(1*H*)-quinolone derivatives to give the corresponding *O*-benzoylsalicylic and anthranilic acid derivatives with concomitant release of carbon monoxide and thus serve as one of the first biomimetic functional models with relevance to the iron-containing flavonol and the cofactor-independent 3-hydroxy-4(1*H*)-quinolone 2,4-dioxygenases. The relative reactivity order of the substrates are flaH (**2a**) > 1Me-PhquinH (**6**) > 2Me-quinH_2 (**3**) > PhquinH_2 (**5a**). The values of the activation parameters, are very similar to each other, supporting similar, associative-type mechanism (Fig. S2) for the investigated substrates. A reaction mechanism that fits the chemical, spectroscopic, kinetic and thermodynamic data is shown in Scheme 4. In summary: Fe^{III}(*O*-bs)(fla)(salen)-catalyzed dioxygenation of flavonol and 3-hidroxy-quinolone derivatives in DMF has a single electron transfer (SET) mechanism in which the deprotonated substrate with increased basicity reduces the molecular oxygen, initiating further steps including a fast consecutive formation of the trioxametallocycle, which reacts by a nucleophilic addition on the C4 carbon to give the endoperoxide intermediates, that lead to the enzyme-like products. It can be also said that the forming carboxylates such as *O*-benzoylsalicilate, and *N*-anthranilate derivatives as coligands dramatically enhance the reaction rate, which can be explained by the formation of more reactive monodentate iron substrate complexes, which is necessary to the intermolecular electron transfer.

Acknowledgments

The authors are grateful for the financial support of the grant TAMOP-4.2.1/B-09/1/KONV-2010-0003: Mobility and Environment:

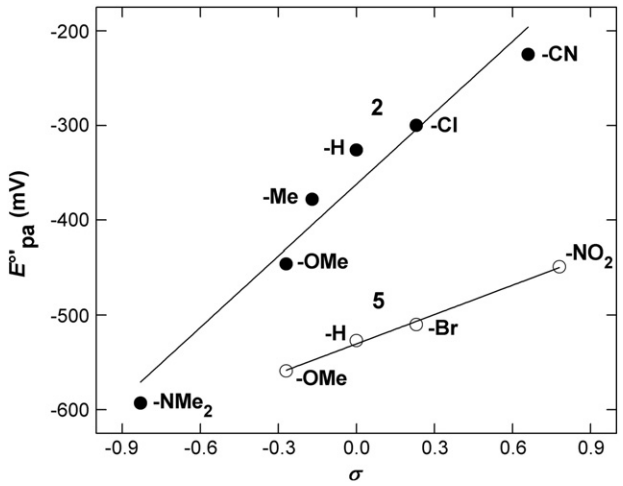

Fig. 6. Correlation between the $E^{\circ\prime}$ potentials and the Hammett's σ for **2** and **5**.

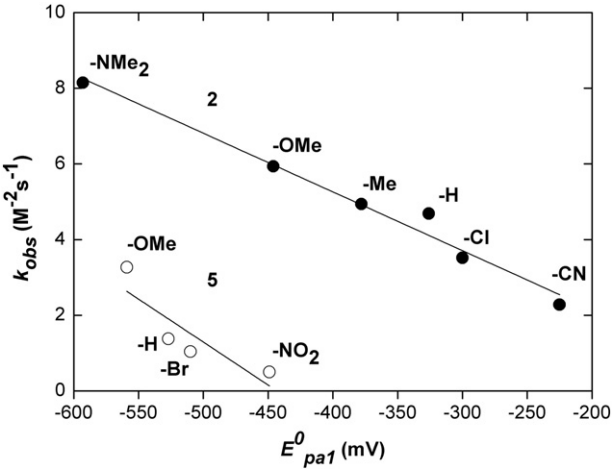

Fig. 7. Dependence of rate constant *k*, on the $E^{\circ\prime}_{pa1}$ for **2** and **5**.

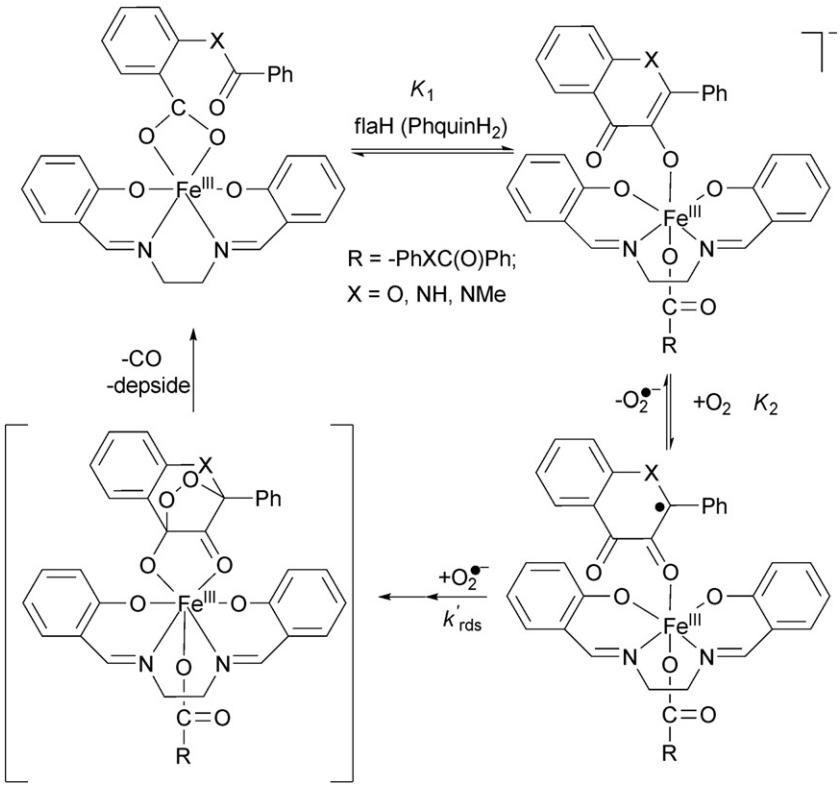

Scheme 4. General mechanism proposal for the catalytic dioxygenation of the various substrates.

Researches in the fields of motor vehicle industry, energetics and environment in the Middle- and West-Transdanubian Regions of Hungary. The project is supported by the European Union and co-financed by the European Regional Development Fund. Financial support of the Hungarian National Research Fund (OTKA K67871, K75783 and PD75360) is also gratefully acknowledged.

Appendix A. Supplementary material

Supplementary data to this article can be found online at doi:10.1016/j.jinorgbio.2011.11.013.

References

[1] E. Wollenweber, in: J.B. Harborne, T.J. Mabry (Eds.), Flavonoids: Advances in Research, Chapman & Hall, London, New York, 1982, p. 189.
[2] J.B. Harborne, C.A. Williams, in: J.B. Harborne, T.J. Mabry (Eds.), Flavonoids: Advances in Research, Chapman & Hall, London, New York, 1982, p. 261.
[3] W. Bors, W. Hellers, C. Michel, Meth. Enzymol. 186 (1990) 343.
[4] Y. Hanasaki, S. Ogawa, S. Fukui, J. Free Radic. Biol. Med. 16 (1992) 605.
[5] J.P. Hu, M. Calomme, A. Lasure, T. De Bryune, L. Pieters, A. Vlietnick, D.D.A. Van den Berghe, Biol. Trace Elem. Res. 47 (1995) 327.
[6] C.A. Rice-Evans, N.J. Miller, G. Pananga, J. Free Radic. Biol. Med. 20 (1996) 933.
[7] A. Gulsen, D.P. Makris, P. Kefalas, Food Res. Int. 40 (2007) 7.
[8] M.G.L. Hertog, E.J.M. Feskens, P.C.H. Hollman, M.B. Katan, D. Kromhout, Lancet 342 (1993) 1007.
[9] H.-K. Hund, A. de Beyer, F. Lingens, Biol. Chem. Hoppe Seyler 371 (1990) 1005.
[10] G. Bott, M. Schmidt, T.O. Rommel, F. Lingens, Biol. Chem. Hoppe Seyler 371 (1990) 999.
[11] S. Fetzner, R.A. Steiner, Appl. Microbiol. Biotechnol. 86 (2010) 791.
[12] E.C. Pesci, J.B.J. Milbank, J.P. Pearson, S. McKnight, A.S. Kende, E.P. Greenberg, B.H. Iglewski, Proc. Natl Acad. Sci. USA 96 (1999) 11234.
[13] S.P. Diggle, P. Cornelis, P. Williams, M. Camara, Int. J. Med. Microbiol. 296 (2006) 83.
[14] J.F. Dubern, S.P. Diggle, Mol. Biosyst. 4 (2008) 882.
[15] T. Oka, F.J. Simpson, Biochem. Biophys. Res. Commun. 43 (1971) 1.
[16] H.-K. Hund, J. Breuer, F. Lingens, J. Hüttermann, R. Kappl, S. Fetzner, Eur. J. Biochem. 263 (1999) 871.
[17] F. Fusetti, K.H. Schröter, R.A. Steiner, P.I. van Nort, T. Pijning, H.J. Rozeboom, K.H. Kalk, M.R. Egmond, B.W. Dijkstra, Structure 10 (2002) 259.
[18] B. Gopal, L.L. Madan, S.F. Betz, A.A. Kossiakoff, Biochemistry 44 (2005) 193.
[19] B.M. Barney, M.R. Schaab, R. LoBrutto, W.A. Francisco, Protein Expr. Purif. 35 (2004) 131.
[20] L. Bowater, S.A. Fairhurst, V.J. Just, S. Bornemann, FEBS Lett. 557 (2004) 45.
[21] R. Qi, S. Fetzner, A.J. Oakley, Acta Crystallogr, Sect. F. 63 (2007) 378.
[22] R.A. Steiner, U. Frerichs-Deeken, S. Fetzner, acta Crystallogr, Sect. F. 63 (2007) 382.
[23] S. Fetzner, Appl. Microbiol. Biotechnol. 60 (2002) 243.
[24] F. Fischer, S. Fetzner, FEMS Microbiol. Lett. 190 (2000) 21.
[25] U. Frerichs-Deeken, K. Ranguelova, R. Kappl, J. Hüttermann, S. Fetzner, Biochemistry 43 (2004) 14485.
[26] É. Balogh-Hergovich, J. Kaizer, G. Speier, G. Argay, L. Párkányi, J. Chem. Soc. Dalton Trans. (1999) 3847.
[27] É. Balogh-Hergovich, J. Kaizer, G. Speier, G. Huttner, A. Jacobi, Inorg. Chem. 39 (2000) 4224.
[28] J. Kaizer, É. Balogh-Hergovich, M. Czaun, T. Csay, G. Speier, Coord. Chem. Rev. 250 (2006) 2222.
[29] J. Kaizer, G. Baráth, J. Pap, G. Speier, M. Giorgi, M. Réglier, Chem. Commun. (2007) 5235.
[30] J.S. Pap, J. Kaizer, G. Speier, Coord. Chem. Rev. 254 (2010) 781.
[31] L. Barhács, J. Kaizer, G. Speier, J. Org. Chem. 65 (2000) 3449.
[32] G. Baráth, J. Kaizer, G. Speier, L. Párkányi, E. Kuzmann, A. Vértes, Chem. Commun. (2009) 3630.
[33] M. Czaun, G. Speier, Tetrahedron Lett. 43 (2002) 5961.
[34] A. Nishinaga, T. Tojo, H. Tomita, T.J. Matsuura, J. Chem. Soc. Perkin Trans. 1 (1979) 2511.
[35] M.A. Smith, R.M. Newman, R.A. Webb, J. Heterocycl. Chem. 5 (1968) 425.
[36] P. Hradil, J. Jirman, Collect. Czech. Chem. Commun. 60 (1995) 1357.
[37] F. Arndt, Organic Syntheses, in: A.H. Blatt (Ed.), John Wiley & Sons, New York, 1943, p. 165.
[38] The Manipulation of Air-Sensitive Compounds, in: D.F. Shriver, M.A. Drezdzon (Eds.), John Wiley & Sons, New York, 1986.
[39] E.G. Samsel, K. Srinivasan, J.K. Kochi, J. Am. Chem. Soc. 107 (1985) 7606.
[40] G.M. Sheldrick, SHELXL97, Program for the Refinement of Crystal Structures, Univ. of Göttingen, Germany, 1997.
[41] A. Kruis, Landolt-Börnstein, Board 4, Teil 4, Springer-Verlag, Berlin, 1976, p. 269.
[42] G. Ram, A.R. Sharaf, J. Ind. Chem. Soc. 45 (1968) 13.
[43] J. Kaizer, S. Góger, G. Speier, M. Réglier, M. Giorgi, Inorg. Chem. 9 (2006) 251.
[44] J. Kaizer, T. Csay, M. Czaun, G. Speier, M. Réglier, M. Giorgi, Inorg. Chem. 8 (2005) 813.
[45] B.H.J. Bielski, H.W. Richter, J. Am. Chem. Soc. 99 (1977) 8085.
[46] J. Kaizer, I. Ganszky, G. Speier, A. Rockenbauer, L. Korecz, M. Giorgi, M. Réglier, S. Antonczak, J. Inorg. Biochem. 101 (2007) 893–899.
[47] I. Ganszky, J. Kaizer, M. Czaun, G. Speier, L. Párkányi, Z. Kristallogr, NCS 222 (2007) 259–260.